

Carbon doped InAlAs/InGaAs/InAs heterostructures: Tuning from n- to p-doping

M. Hirmer, D. Schuh, and W. Wegscheider

Citation: *Appl. Phys. Lett.* **98**, 082103 (2011); doi: 10.1063/1.3557026

View online: <http://dx.doi.org/10.1063/1.3557026>

View Table of Contents: <http://apl.aip.org/resource/1/APPLAB/v98/i8>

Published by the [American Institute of Physics](#).

Related Articles

Role of surface trap states on two-dimensional electron gas density in InAlN/AlN/GaN heterostructures
Appl. Phys. Lett. **100**, 152116 (2012)

Free carrier accumulation at cubic AlGaIn/GaN heterojunctions
Appl. Phys. Lett. **100**, 142108 (2012)

Influence of La and Mn dopants on the current-voltage characteristics of BiFeO₃/ZnO heterojunction
J. Appl. Phys. **111**, 074101 (2012)

Ge/SiGe heterostructures as emitters of polarized electrons
J. Appl. Phys. **111**, 063916 (2012)

Gate metal induced reduction of surface donor states of AlGaIn/GaN heterostructure on Si-substrate investigated by electroreflectance spectroscopy
Appl. Phys. Lett. **100**, 111908 (2012)

Additional information on *Appl. Phys. Lett.*

Journal Homepage: <http://apl.aip.org/>

Journal Information: http://apl.aip.org/about/about_the_journal

Top downloads: http://apl.aip.org/features/most_downloaded

Information for Authors: <http://apl.aip.org/authors>

ADVERTISEMENT



GET YOUR COPY TODAY >>

**FREE CD with 700
Multiphysics Presentations**

COMSOL

Carbon doped InAlAs/InGaAs/InAs heterostructures: Tuning from n- to p-doping

M. Hirmer,^{1,a)} D. Schuh,¹ and W. Wegscheider^{1,2}

¹*Institut für Experimentelle und Angewandte Physik, Universität Regensburg, D-93040 Regensburg, Germany*

²*Laboratorium für Festkörperphysik, ETH Zürich, Schafmattstr. 16, 8093 Zürich, Switzerland*

(Received 17 December 2010; accepted 1 February 2011; published online 22 February 2011)

We fabricated carbon doped InAs/In_xGa_{1-x}As/In_xAl_{1-x}As heterostructures, which show p-type and n-type conductivity for different In contents. Two-dimensional hole gas in a structure with $x=0.75$ has been prepared in the ternary compound, despite the fact that carbon as an n-type dopant in InAs exhibits electron conductivity in In_xGa_{1-x}As and In_xAl_{1-x}As compounds with high indium content. A special doping design has been employed to obtain hole conductivity. As a result, the conductivity can be tuned from n-type to p-type with the In content and with different doping profiles in these structures. © 2011 American Institute of Physics. [doi:10.1063/1.3557026]

Currently, a lot of attention is directed to In_xGa_{1-x}As/In_xAl_{1-x}As heterostructures due to their interesting properties, such as low electron effective mass, high electron mobility, high g-factor, narrow gap, pronounced Rashba effect due to high spin-orbit coupling.¹⁻³ They are used for the design of hybrid metal-semiconductor structures with highly transmissive interfaces,^{4,5} tunable spin filters,⁶ or spin transistors.⁷ Also the strain due to the lattice mismatch in In-containing GaAs/AlGaAs structures can be employed as additional degree of freedom in bandgap engineering.⁸

The concept of a step-graded metamorphic buffer layer with gradually increasing indium content, see, e.g., Heyn *et al.*,⁹ made it possible to grow almost unstrained In_xGa_{1-x}As/In_xAl_{1-x}As heterostructures with high indium content on GaAs substrates. Two-dimensional electron gases in In_{0.75}Ga_{0.25}As/In_{0.75}Al_{0.25}As heterostructures with embedded InAs channel can be achieved in undoped^{10,11} and silicon doped structures.¹² They show high electron mobilities¹³ of up to $\mu=545\,000\text{ cm}^2/\text{V s}$. Apart from Mn-modulation doping, which leads to interesting magnetic effects,¹⁴ there have been no reports on hole conductivity in modulation-doped structures. Carbon as a doping material regularly used in GaAs-based heterostructures is a very promising candidate. Since, it exhibits very low diffusion and segregation,¹⁵ it is possible to achieve very high hole mobilities of up to $1.2 \times 10^6\text{ cm}^2/\text{V s}$ at low temperatures in carbon p-type doped GaAs/AlGaAs heterostructures.¹⁶

Here, we present our results on In_xGa_{1-x}As/In_xAl_{1-x}As heterostructures prepared in a modified Veeco GEN II solid source molecular beam epitaxy system, equipped with a carbon filament source. On a semi-insulating (100) GaAs substrate we have grown an In_xAl_{1-x}As step-graded metamorphic buffer layer with stepwise ($\Delta x=0.05$) increasing indium content from $x=0.08$ up to the final composition $x=0.40$, 0.50, 0.60, or 0.75. Within each 50 nm thick In_xAl_{1-x}As step, the lattice constant relaxes due to misfit dislocation formation. The active layer consists of an In_xAl_{1-x}As barrier, a 20 nm In_xGa_{1-x}As single quantum well (QW) with embedded strained InAs channel, In_xAl_{1-x}As spacer layer, carbon doping layer, In_xAl_{1-x}As cap layer [see sample structure in Fig.

1(a)]. We used two different doping techniques: modulation doping in the In_xAl_{1-x}As layer for active layers with $x=0.20$, 0.40, 0.50, 0.60, and 0.75 and digital-alloy doping for the active layer with $x=0.75$. In the second case, utilizing the fact that carbon acts as an acceptor in In_xGa_{1-x}As and In_xAl_{1-x}As with low indium content, we grew one layer In_{0.75}Al_{0.25}As, one layer AlAs, both homogeneously doped with carbon, and a carbon δ -doping layer and repeated this layer sequence four-times. This gives an overall indium content of $x=0.40$ in the doping layer. The growth rate was $1.2\text{ }\mu\text{m/h}$ under As₄-rich conditions and the substrate tem-

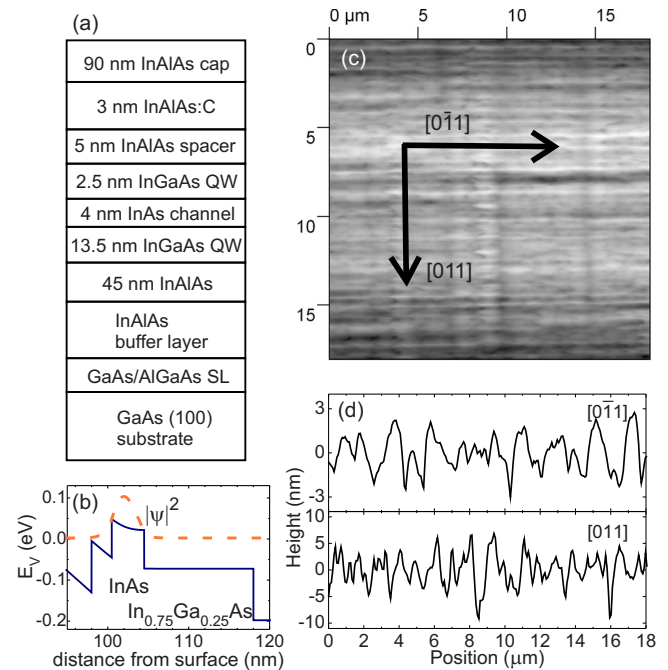


FIG. 1. (Color online) (a) Example of the sample structure. Shown is the layer sequence for the sample with $x=0.75$ indium in the active layer and p-type conductivity. (b) Calculated valence band profile and square of hole wave function shifted to its eigenvalue (dashed line) of the digitally-doped sample with $x=0.75$. Band energies E_V are relative to the Fermi energy. (c) AFM image of the surface of the structure with $x=0.75$ In, containing a 2DHG. It exhibits a typical cross-hatched pattern. (d) Height profiles along the [011] and [0 $\bar{1}$ 1] crystal directions.

^{a)}Electronic mail: marika.hirmer@physik.uni-regensburg.de.

TABLE I. Magnetotransport measurement results of $\text{In}_x\text{Al}_{1-x}\text{As}/\text{In}_x\text{Ga}_{1-x}\text{As}/\text{InAs}$ heterostructures at 4.2 K without illumination. (Positive carrier density stays for holes and negative for electrons.)

Indium content $x=$	Carrier density ($\times 10^{11} \text{ cm}^{-2}$)	Carrier mobility ($\times 10^3 \text{ cm}^2/\text{V s}$)
0.20	15.2	1.8
0.40	6.5	2.0
0.50	11.7	1.7
0.60	11.9	3.7
0.75 (modulation doped)	-1.7	12.1
0.75 (digitally doped)	12.2	6.0

perature was kept at 620 °C during the growth of the $\text{Al}_{0.5}\text{Ga}_{0.5}\text{As}/\text{GaAs}$ superlattice, and lowered to 340 °C for the indium containing layers. Figure 1(b) shows valence band profile and square of hole wave function $|\psi|^2$, shifted to its eigenvalue, of the digitally-doped sample with $x=0.75$, see also Table I, calculated with the NEXTRANO3 program package¹⁷ using effective-mass approximation method. Despite the high hole density of $p > 10^{12} \text{ cm}^{-2}$, only the topmost subband in the valence band is occupied. Two-dimensional hole gas (2DHG) is situated in the InAs channel.

To study the morphological properties of the surface of the grown crystals, we used an atomic force microscope (AFM). The surface of all samples exhibits a well-developed cross-hatched pattern along the two orthogonal $\langle 011 \rangle$ directions, as shown in Fig. 1(c). This typical property originates from misfit dislocations buried in the buffer layer.^{11,18} The root mean square roughness is 1.2 nm along the $[0\bar{1}1]$ direction and 2.9 nm along the $[011]$ crystal direction, as can be seen in Fig. 1(d). No significant differences were found between samples with different indium content.

The electrical characterization of the samples was performed in van der Pauw and Hall bar geometry using standard lock-in techniques at low temperatures (4.2 K, 1.3 K, and 280 mK).

The electrical properties of the modulation-doped samples are summarized in Fig. 2 and Table I. In Fig. 2(a), the carrier density is shown as a function of the indium content x in the active layer. The samples with $x=0.20$ to 0.60 indium show hole conductivity. The sample with the highest indium content of $x=0.75$ exhibits electron conductivity. Thus, the carrier type changes between $x=0.60$ and $x=0.75$ for modulation doping in $\text{In}_x\text{Al}_{1-x}\text{As}$. This is in contrast to literature showing for the strained bulk $\text{In}_x\text{Al}_{1-x}\text{As}$ and $\text{In}_x\text{Ga}_{1-x}\text{As}$, grown on (100) GaAs substrates without buffer layer, conduction type inversion from p to n at $x=0.9$ for $\text{In}_x\text{Al}_{1-x}\text{As}$ and at $x=0.6$ for $\text{In}_x\text{Ga}_{1-x}\text{As}$.¹⁹ The difference to our samples can originate from the different sample structure, containing the buffer layer which relaxes the strain in our case, and could lead to another incorporation mechanism.

In Fig. 2(b), the carrier density is plotted as a function of the carbon doping concentration in samples with $x=0.75$ in the active layer. The thickness of the doping layer was kept constant at 90 nm. With increasing doping intensity, the electron density also increases. Hence, it is not possible to obtain hole conductivity by only incorporating more carbon atoms into the layer. Illumination with a red light emitting diode induces an increase in the electron density at low carbon

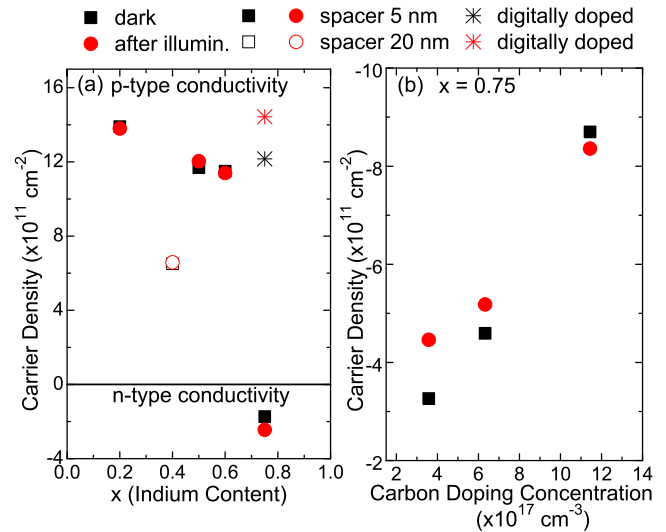


FIG. 2. (Color online) (a) Carrier density as a function of indium content in the active layer and (b) electron density in dependence on doping concentration in the sample with $x=0.75$ indium content, measured at 4.2 K before and after illumination.

doping concentrations and a reduction at high doping concentrations [Fig. 2(b)]. This is a sign of self-compensation of carbon atoms at high doping densities. Carbon has been reported to be a donor in InAs (Refs. 19 and 20) and InP.²¹ But, as a group IV member, carbon behaves amphoteric for III-V semiconductors and shows strong self-compensation behavior in these materials, resulting in conduction type inversion with changing composition.¹⁹

Using a carbon digital-alloy-doping technique, we overcame this problem and obtained hole conductivity in the $\text{In}_{0.75}\text{Al}_{0.25}\text{As}/\text{In}_{0.75}\text{Ga}_{0.25}\text{As}/\text{InAs}$ heterostructure. The sample has a hole density of $p=11.4 \times 10^{11} \text{ cm}^{-2}$ and a hole mobility of $\mu=6.6 \times 10^3 \text{ cm}^2/\text{V s}$ at 280 mK. In Fig. 3, magnetotransport measurements at low temperatures (280 mK) are displayed. The positive slope of the Hall curve R_{xy} confirms the hole conductivity. The Hall resistance R_{xy} demonstrates well-developed plateaus at even filling factors. The longitudinal resistance R_{xx} exhibits well-pronounced Shubnikov–de Haas oscillations already at 1.3 K, which are not observable at this temperature when high mobility

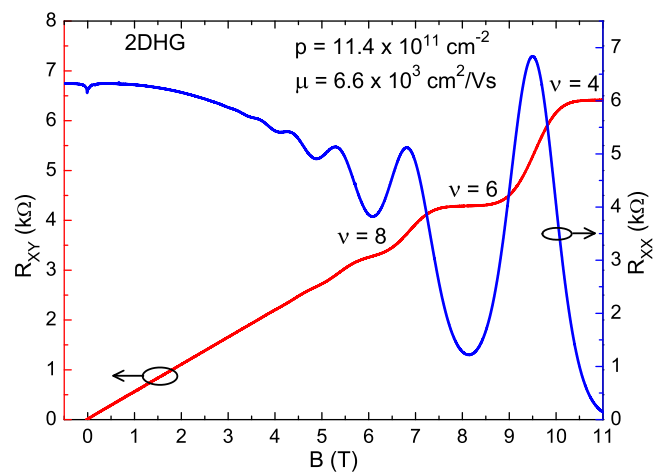


FIG. 3. (Color online) Magnetotransport measurements at 280 mK on the digitally-doped sample with $x=0.75$ in the active layer showing p-type conductivity, without illumination.

2DHGs in GaAs/AlGaAs QWs are measured.²² A possible explanation is the lower hole effective mass in InAs ($m_h^* = 0.39 m_0$) (Ref. 23) in comparison with GaAs ($m_h^* = 0.51 m_0$, m_0 is the free electron mass).²³ The small decrease in the longitudinal resistance around $B=0$ T, already observable at 4.2 K, could be classified as a weak antilocalization dip, due to strong spin-orbit coupling in InAs. 2DHGs formed by Mn-modulation doping show a similar effect.¹⁴

In conclusion, we grew carbon doped $\text{In}_x\text{Ga}_{1-x}\text{As}/\text{In}_x\text{Al}_{1-x}\text{As}$ heterostructures, which show p-type conductivity in a large range of In content. Although carbon seems to be a donor in InAs, our concept of doping makes it possible to produce 2DHGs also in structures with high indium content ($x=0.75$). The sample exhibits quantized Hall plateaus, well-pronounced Shubnikov–de Haas oscillations, and a weak antilocalization dip around zero magnetic field.

We thank U. Wurstbauer, W. Hansen for discussions, and I. Gronwald for AFM pictures. We acknowledge financial support by the Deutsche Forschungsgemeinschaft (DFG) via SFB 689, SFB 631, and BMBF Förderschwerpunkt Nano-QUIT.

- ¹C. Hermann and C. Weisbuch, *Phys. Rev. B* **15**, 823 (1977).
²C. H. Möller, C. Heyn, and D. Grundler, *Appl. Phys. Lett.* **83**, 2181 (2003).
³D. Grundler, *Phys. Rev. Lett.* **84**, 6074 (2000).
⁴C. H. Möller, O. Kronenwerth, D. Grundler, W. Hansen, C. Heyn, and D. Heitmann, *Appl. Phys. Lett.* **80**, 3988 (2002).
⁵M. Holz, O. Kronenwerth, and D. Grundler, *Phys. Rev. B* **67**, 195312

- (2003).
⁶M. J. Gilbert and J. P. Bird, *Appl. Phys. Lett.* **77**, 1050 (2000).
⁷S. Datta and B. Das, *Appl. Phys. Lett.* **56**, 665 (1990).
⁸R. Schuster, H. Hajak, M. Reinwald, W. Wegscheider, D. Schuh, M. Bichler, and G. Abstreiter, *Appl. Phys. Lett.* **85**, 3672 (2004).
⁹C. Heyn, S. Mendach, S. Löhr, S. Beyer, S. Schnüll, and W. Hansen, *J. Cryst. Growth* **251**, 832 (2003).
¹⁰F. Capotondi, G. Biasiol, I. Vobornik, L. Sorba, F. Giazotto, A. Cavallini, and B. Fraboni, *J. Vac. Sci. Technol. B* **22**, 702 (2004).
¹¹F. Capotondi, G. Biasiol, D. Ercolani, V. Grillo, E. Carlino, F. Romanoto, and L. Sorba, *Thin Solid Films* **484**, 400 (2005).
¹²A. Richter, M. Koch, T. Matsuyama, C. Heyn, and U. Merkt, *Appl. Phys. Lett.* **77**, 3227 (2000).
¹³S. Gozu, T. Kita, Y. Sato, S. Yamada, and M. Tomizawa, *J. Cryst. Growth* **227–228**, 155 (2001).
¹⁴U. Wurstbauer, D. Schuh, D. Weiss, and W. Wegscheider, *Physica E* **42**, 1145 (2010).
¹⁵N. Kobayashi, T. Makimoto, and Y. Horikoshi, *Appl. Phys. Lett.* **50**, 1435 (1987).
¹⁶C. Gerl, S. Schmult, H.-P. Tranitz, C. Mitzkus, and W. Wegscheider, *Appl. Phys. Lett.* **86**, 252105 (2005).
¹⁷S. Birner, S. Hackenbuchner, M. Sabathil, G. Zandler, J. A. Majewski, T. Andlauer, T. Zibold, R. Morschl, A. Trellakis, and P. Vogl, *Acta Phys. Pol. A* **110**, 111 (2006).
¹⁸E. A. Fitzgerald, Y.-H. Xie, D. Monroe, P. J. Silverman, J. M. Kuo, A. R. Kortan, F. A. Thiel, and B. E. Weir, *J. Vac. Sci. Technol. B* **10**, 1807 (1992).
¹⁹H. Ito and T. Ishibashi, *Jpn. J. Appl. Phys., Part 2* **30**, L944 (1991).
²⁰M. Kamp, R. Contini, K. Werner, H. Heinecke, M. Weyers, H. Lüth, and P. Balk, *J. Cryst. Growth* **95**, 154 (1989).
²¹S. J. Pearton, U. K. Chakrabarti, C. R. Abernathy, and W. S. Hobson, *Appl. Phys. Lett.* **55**, 2014 (1989).
²²J. J. Heremans, M. B. Santos, and M. Shayegan, *Appl. Phys. Lett.* **61**, 1652 (1992).
²³W. Nakwaski, *Physica B* **210**, 1 (1995).